Carbohydrate Polymers 87 (2012) 2129–2136

Contents lists available at SciVerse ScienceDirect

Carbohydrate Polymers

journal homepage: www.elsevier.com/locate/carbpol

Determination of molecular size of O-(2-hydroxyethyl)cellulose (HEC) and its relationship to the mechanism of enzymatic hydrolysis by cellulases

Antonio Martínez-Richa*

Departamento de Química, Universidad de Guanajuato, Noria Alta S/N, 36050 Guanajuato, Gto. Mexico

ARTICLE INFO

Article history:
Received 5 September 2011
Received in revised form 9 October 2011
Accepted 15 October 2011
Available online 20 October 2011

Keywords:
Chain dimensions
O-(2-hydroxyethyl)cellulose (HEC)
Enzymatic hydrolysis by cellulases
Flory exponent
Persistence length

ABSTRACT

Z-average root mean square end-to-end distance $\langle r_o^2\rangle_z^{1/2}$ and radius of gyration $\langle s_o^2\rangle_z^{1/2}$ for 13 samples of O-(2-hydroxyethyl)cellulose (HEC) of different molecular weights were derived from Gel Permeation Chromatography and intrinsic viscosity measurements with water as a solvent. At 40 °C and pH 4.5, contraction of chain dimensions is observed, compared with the sizes observed under neutral conditions at room temperature. The effect is lower for samples with higher molecular weights. Values of $\langle r_o^2\rangle_{40}/DP_z$ also indicate that chain flexibility increases at higher temperature and acidic conditions. From the analysis of molecular weight dependence of $\langle s_o^2\rangle_z^{1/2}$, Flory exponent υ was derived at 40 °C and pH 4.5. A value of $\upsilon = 0.70 \pm 0.02$ was recorded, which indicates that a relatively stiff chain is present under these conditions. Finally, different equations to calculate persistence length L_p were evaluated. Values in the range of 260–400 Å were derived for persistence length. Implications of chain conformation in the enzymatic action of cellulases are also discussed.

1. Introduction

Cellulose-based derivatives are an important class of polymers with a variety of industrial applications. They are in general obtained heterogeneously by the reaction of cellulose with alkali and then treating with an appropriate derivative. In particular, O-(2-hydroxyethyl)cellulose HEC – an important water-soluble polymer – is produced by the reaction of alkali cellulose with ethylene oxide (Majewicz, Erazo-Majewicz, & Podlas, 2005). HEC is an important non-ionic biodegradable polysaccharide that has interesting hydrophilic, rheological and antibacterial properties. Its commercial applications involve aqueous solutions, and based on its properties it can act as a thickener or binder, or as a protective colloid and suspension stabilizer. HEC possesses an excellent salt compatibility, and transparent films are easily achieved from aqueous solutions.

Substituent distribution on HEC is statistical in nature. The β-D-anhydroglucopyranose (AHG) moiety of cellulose possesses one primary hydroxyl group at the carbon-6 position and two secondary hydroxyl groups at carbons 2 and 3. These residues react with ethylene oxide to yield 2-hydroxyethyl substituents, which contain a terminal primary hydroxyl. The 2-hydroxyethyl substituents can, in turn, react with more ethylene oxide to form pendant poly(ethylene glycol) side chains. Since pendant groups are formed, the degree of substitution (DS, that reflects the average number of substituent groups per anhydroglucose unit) is lesser than the molar substitution (MS) (see Fig. 1).

The physicochemical and functional properties of O-(2-hydroxyethyl)cellulose (HEC) depend on the conformational characteristics of the individual chains along with their ability to interact in solution and in the solid state. In solution, HEC presents a versatile conformation influenced by pH, ionic strength, temperature and other factors. As distribution of substituents along the AHG determines most of the HEC properties; the desirable physical properties are achieved by the obtainment of a predetermined substituted derivative (Majewicz et al., 2005). However, the challenge is to find ways of modifying polysaccharides so that biodegradability is not lost (Roesser, McCarthy, Gross, & Kaplan, 1996).

The use of biodegradation to break down cellulose and its derivatives is commonly used in the textile, wood-pulp and other industries. Efforts are directed toward the replacement of energy intensive processes, as well as to the development of new methods of biodegradation of wastes with the possibility of recycling (Brennan, 1998). Hydroxyethylcellulose (HEC) represents an important model system to study the effect of cellulose modification on enzymatic degradation.

Cellulase enzyme assay is commonly used to evaluate resistance toward enzymatic degradation of cellulose derivatives. The most important factor that determines the rate of enzymatic hydrolysis is the degree of substitution. However, site of substitution and molecular size are important when systems of similar degree of substitution are compared. Correlations between the degree of

---

* Tel.: +52 473 7320006x1411.
E-mail address: richa@ugto.mx

0144-8617/$ – see front matter © 2011 Elsevier Ltd. All rights reserved.
doi:10.1016/j.carbpol.2011.10.039

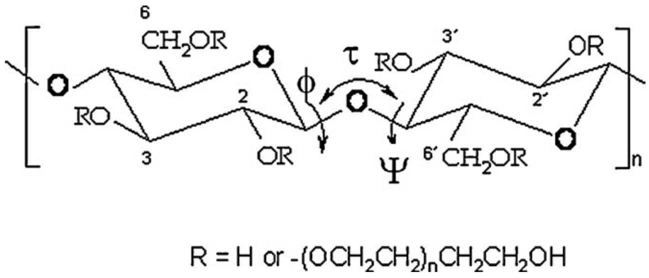

Fig. 1. Chemical structure for O-(2-hydroxyethyl)cellulose (HEC), showing the important atom labels. Torsion angles Φ and ψ and covalent glycosidic linkage bond angle τ are defined as shown.

substitution, site of substitution, molecular size and degradation for some cellulose derivatives has been derived (Brennan, 1998; Klop & Kooiman, 1965; Klug, Winquist, & Lewis, 1973; Martínez-Richa, Muñoz-Alarcón, & Joseph-Nathan, 1992; Martínez-Richa, 1998; Tezuka, Imai, Oshima, & Chiba, 1989; Wirick, 1968).

Chain dimensions of O-(2-hydroxyethyl)cellulose (HEC) depend upon factors such as pH, solvent, temperature, ionic force, etc. In neutral aqueous solutions and at room temperature, HEC acquires a rigid chain and highly extended shape. This configuration is mainly due to the existence of molecular packing of solvent molecules around polymer chain that restrict rotations of the repeating units. At higher temperatures and under basic or acidic conditions, chain flexibility increases and molecular size is smaller (Brown, Henley, & Ohman, 1963).

Mechanism of enzyme action on cellulose and cellulose derivatives involves chain scission mainly between pairs of adjacent unsubstituted anhydroglucose (AHG) units. Additional chain scissions also occur when sequences of unsubstituted and only substituted at position-6 residues exists as well (Klop & Kooiman, 1965; Martínez-Richa et al., 1992; Martínez-Richa, 1998). In a previous work, comparative studies of the biodegradability of HEC samples were made by the exposure of these polymers to enzyme Celulex-123 (liquid cytolase enzyme) (Martínez-Richa et al., 1992). It was found that both degree of substitution and molecular size are related with enzymatic resistance of HEC to cellulases.

Eventhough the effect of pH and temperature on HEC solutions is well known (Brown et al., 1963), a comprehensive characterization of physicochemical parameters associated with chain dimensions (including the calculation of important parameters such as Flory exponent and persistence length L_p) of these polymers has not been undertaken. In this work, experimental results obtained from GPC and viscosity measurements are presented. Special emphasis is made to calculate the above-mentioned parameters for the conditions used to determine the enzymatic resistance of HEC to cellulases. Complete information on the chain size for several samples of HEC were derived at room temperature and at pH 4.5 and 40 °C. Results are analyzed in the light of the factors that influence biodegradation of HEC by cellulases.

1.1. Theoretical considerations

1.1.1. Description of polymer chain in polysaccharides

Polymer chain can adopt many different configurations in solution. Rod-like, spherical, and extended chain configurations are commonly observed as a function of solution parameters (Katime and Cesteros, 2004; Sun, 2004; Teraoka, 2002). Observed polymer configuration is linked with local conformations, which depends on torsion rotations about carbon–carbon bonds present in the polymer backbone. Conformational changes are responsible for the observed polymer shapes, which in turn are associated with changes in macroscopic physicochemical properties.

The schematic representation of the dimer repeat unit chemical structure for HEC is displayed in Fig. 1. The differences among the various forms of cellulose derivatives include chain packing, primary alcohol orientation, hydrogen bonding nature and the shape of the glucose rings. Primary structure of polysaccharides depends on many factors such as linkage positions between AHG units ($1 \rightarrow 2, 1 \rightarrow 3, 1 \rightarrow 4$, etc.) and anomeric forms (α or β). The so-called secondary structure depends on the conformation present along the polysaccharide backbone. The secondary structure is defined by the amount of rotation along the torsion angles ψ and Φ about the glycosidic linkages, and in a lesser extent by the covalent glycosidic linkage bond angle τ (see Fig. 1) (French & Johnson, 2004; Saito, Tuzi, & Naito, 1998). In Fig. 1, Φ is defined as O–C1–O–C4′, ψ as C1–O–C4′–C5′ and τ as C1–O–C4′. Derivation of 3-D structure for polysaccharides from lowest energy conformers lead to the formation of extended helices (French, Kelterer, Johnson, Dowd, & Cramer, 2000; Mazeau, Moine, Krausz, & Gloaguen, 2005). Polysaccharide conformation depends on the environment surrounding the polymer chain, and a broad variety of molecular shapes have been found in celluloses derivatives (French & Johnson, 2004). Observance of extended single or multiple helical chains are related with changes in the secondary structure.

Barriers to bond rotations about torsion angles ψ and Φ are high in polysaccharides. For cellulose derivatives, this places severe conformational restrictions on the cellulose chains, which results in efficient packing and strong interaction between cellulose chains. An extensive interchain hydrogen-bonding between hydroxyl groups is present (French & Johnson, 2004; Tonelli, 2001). Molecular dimensions calculated for cellulose using conformational energy maps $E(\psi,\Phi)$ confirms that a highly extended rigid structure is characteristic of this polymer and its derivatives (Brant & Christ, 1990, chap. 4).

1.1.2. Thermodynamic behavior of dilute cellulose derivatives solutions

Due to the low chain flexibility of anhydroglucose chains, the behavior of cellulose derivatives in solution is markedly different from that of flexible polymers. A higher degree of rotation along the glycosidic bonds reduces chain dimensions through an increase of chain flexibility. So, smaller dimensions are observed in good solvents compared to those under theta conditions (Brown et al., 1963).

Parameters useful to characterize the configurational characteristics of polymer chains are (1) end-to-end distance $\langle r^2\rangle^{1/2}$ and (2) radius of gyration $\langle s^2\rangle^{1/2}$ (Katime and Cesteros, 2004; Sun, 2004; Teraoka, 2002; Tonelli, 2001). $\langle r^2\rangle^{1/2}$ and $\langle s^2\rangle^{1/2}$ are measures of the size of polymer averaged over all available polymer conformations.

Short-range steric interactions between neighboring or near-neighboring polymer segments dictate macromolecular size. This on turn depends on polymer molecular weight. One important experimentally measured parameter is the intrinsic viscosity $[\eta]$. Intrinsic viscosity measured at θ temperature or in poor solvents, $[\eta]_\theta$, is proportional to the ratio of effective hydrodynamic volume of the polymer to its molecular weight M (Sun, 2004).

$$[\eta]_\theta \sim \frac{\langle r^2\rangle^{1/2}}{M} \tag{2}$$

Introducing the universal constant Φ in Eq. (2), the following relationship between $[\eta]_\theta$ and molecular weight can be derived (Flory–Fox equation) (Flory & Fox, 1951):

$$[\eta]_\theta \sim \frac{\langle r^2\rangle^{3/2}}{M} = \Phi\left(\frac{\langle r\rangle^2}{M}\right)^{3/2} M^{1/2} \tag{3}$$

In this equation, Φ is $\approx 2\times10^{21}$ dl/g mol cm^3, $\langle r_o\rangle^2$ and $\langle r^2\rangle$ are the mean root square of the end-to-end distance for unperturbed and perturbed chains, respectively, and M is the molecular weight.

Under perturbed conditions, this equation takes the form

$$[\eta] = \Phi\frac{\langle r^2\rangle^{3/2}}{M} = \Phi\left(\frac{\langle r_{o^2}\rangle}{M}\right)^{3/2} M^{1/2}\alpha^3 \tag{4}$$

where α is the chain expansion coefficient. For HEC, α can be calculated from Orofino–Flory equation (Brown et al., 1963; Orofino & Flory, 1957):

$$A_2 = \left(\frac{16\pi}{3^{3/2}}\right)\left(\frac{N_A\langle s^2\rangle z^{3/2}}{Mz^2}\right)\ln\left[1+\frac{\pi^{1/2}}{2}(\alpha^2-1)\right] \tag{5}$$

where A_2 (the second virial coefficient) depends on solvent, temperature and weight-average molecular weight. In aqueous solutions, $A_2 = 190\,\mathrm{DP_w}^{-0.48}$. α is close to unit and exhibit a negligible variation on molecular weight (Brown et al., 1963).

Other important parameters for HEC are the effective bond length b, calculated as

$$b = \left(\frac{\langle r_{o^2}\rangle}{DP_z}\right)^{1/2} \tag{6}$$

and the Kuhn–Kuhn equivalent chain length A_m, which for HEC can be computed using the Eq. (7) (Brown et al., 1963).

$$A_m = 1.94\times10^7\left(\frac{\langle r_{o^2}\rangle}{DP_z}\right) \tag{7}$$

From this value, the number of monomer units can be obtained, considering that the length of anhydroglucose unit is 5.04 Å (French & Johnson, 2004).

1.1.3. *Characteristic ratio and Flory exponent ν*

The characteristic ratio of a polymer C_n, calculated by the ratio of $\langle r^2\rangle_0$ to the number of bonds n multiplied by the square of the bond length

$$C_n = \frac{\langle r^2\rangle_0}{nl^2} \tag{8}$$

is an estimation of the polymer chain stiffness. If the effective bond length b and the number of monomer units of the Kuhn–Kuhn equivalent chain length A_m are known, C_n can be calculated using the equivalent equation $C_n = \langle r^2\rangle_0/n'b^2$, where n' is the ratio DP_z/A_m.

Dependence of root mean square end-to-end distance and radius of gyration on molecular weight is generally represented by an exponential equation of the form

$$\langle s_{o^2}\rangle^{1/2} = bN^{\nu} \tag{9}$$

where ν represents the Flory exponent, and represents an excluded-volume term (Teraoka, 2002).

For random coils, ν is 0.5 for polymers in theta conditions (Gaussian polymers) and 0.6 in good solvents (Sun, 2004; Flory, 1969). For rodlike molecules, $\langle s_o{}^2\rangle^{1/2} = bN$. Intermediate values are observed in systems such as polymeric two-dimensional films, where ν in the range 0.75–0.79 are common (Eisenriegler, 1993; Ferenczi & Cicuta, 2005; Flory, 1971; Tatek & Slater, 2006). Flory exponent ν depends on polymer stiffness, and in its mean-field approximation depends on the parameter d, which is the dimension of the physical space to which the polymer is confined (d = 1,2,3,...) (de Gennes, 1979; Flory, 1969; Jaric & Tuthill, 1985; Kamien, 1993; Sun, 2004).

$$\nu = \frac{3}{(d+2)}\ \text{for}\ d < 4 \tag{10}$$

$$\nu = \frac{1}{2}\ \text{for}\ d \geq 4 \tag{11}$$

For rod-like systems, ν approach to the Flory value of 0.75 for two-dimensional polymers (d = 2) (Jaric & Tuthill, 1985).

1.1.4. *Persistence length*

For stiff and semi rigid chains (wormlike chains), a model proposed by Kratky and Porod has been adopted to calculate the chain dimensions of these systems. To describe polymeric chains with backbone rigidity, they introduce the concept of persistence length, L_p, which represents the average projection of the end group on the direction of the first bond (Cifra, 2004).

$$L_p = <\sum_{i=1}^{N-1}\vec{l_i}\,\vec{l_1} > / < / > \tag{12}$$

Persistence lengths can be derived from the relationship between radius of gyration and molecular weight. Rewriting of the Kratky–Porod wormlike chain equation leads to the following expression: (Heine, Kratky, & Porod, 1961; Sun, 2004; Tümmler, Maass, Weber, Wehner, & Vögtle, 1977)

$$\frac{\langle S^2\rangle}{M} = \frac{L_p}{3m_L} - \frac{L_{p^2}}{M} + \frac{2{L_p}^3 m_L}{M^2}\left(1-\frac{L_p m_L}{M}[1-\exp(-M/(L_p\,m_L))]\right) \tag{13}$$

where $m_L = M/L_c$ is the molecular weight per unit contour length. Estimation of both persistence length L_p and m_L can be obtained by non-linear curve-fitting to Eq. (12).

A simplified version of this equation was proposed by H. Murakami, T. Norisuye and H. Fujita (M–N–F model) in 1980: (Murakami, Norisuye, & Fujita, 1980)

$$\left(\frac{M}{\langle s^2\rangle}\right)^{1/2} = \left(\frac{3m_L}{L_p}\right)^{1/2}\left[1+\frac{3L_p m_L}{2M}\right] \tag{14}$$

This equation presents some statistical difficulties as the same variable (M) is used in both, the ordinate and the abscissa; (Mourey, Le, Bryan, Zheng, & Bennet, 2005) however, it provides with a gross estimate of persistence length L_p.

Other equation used to estimate wormlike chain parameters is the linear approximation of the Yamakawa, Fujii and Yoshizaki (YFY) model (Bohdanecky, 1983).

$$\left(\frac{M^2}{[\eta]}\right)^{1/3} = A_n + B_n M^{1/2} \tag{15}$$

where

$$A_n = \frac{A_0 M_L}{\phi_\infty^{1/3}}$$

and

$$B_n = \frac{B}{\phi_{\infty 1/3}}\left(\frac{2L_p}{M_L}\right)^{-1/2}$$

Being $\phi_\infty = 2.87\times10^{23}$, $A_0 = 0.46 - 0.53\ \log\ d_T$ and $B_0 = 1.00 - 0.367\ \log\ d_T$, with $d_T = d/2L_p$. B_0 is a slowly decreasing function of d_T and, to a first approximation, is replaced by its mean value, 1.05.

2. Materials and methods

2.1. *Samples and materials*

The thirteen HEC samples of this study were prepared from ethylene oxide and cellulose (Martínez-Richa et al., 1992; Martínez-Richa, 1998). The MS values were determined by the hydroiodic acid method (Morgan, 1946). The DS values were obtained from the high-resolution Carbon-13 NMR spectra of the samples in D_2O (Tezuka et al., 1989; Martínez-Richa et al., 1992). The samples were treated with warm ethanol (60 °C) by Soxhlet extraction for 72 h before proceeding with the assay. The enzyme

Table 1
Physicochemical parameters for HEC samples at room temperature.

SAMPLE	$M_z \times 10^{-3}$ (daltons)	DP_z	$\langle r^2\rangle_z{}^{1/2} \times 10^{-3}$ (Å)	$\langle s^2\rangle_z{}^{1/2} \times 10^{-3}$ (Å)
HEC-1	681	2770	1.50	0.610
HEC-2	736	3020	1.57	0.640
HEC-3	834	3450	1.61	0.660
HEC-4	906	3620	1.66	0.680
HEC-5	973	3900	1.73	0.710
HEC-6	986	4060	1.76	0.720
HEC-7	1014	4130	1.78	0.730
HEC-8	1042	4170	1.81	0.740
HEC-9	1084	4400	1.83	0.750
HEC-10	1112	4450	1.92	0.780
HEC-11	1278	4700	2.00	0.820
HEC-12	1292	4870	2.03	0.830
HEC-13	1320	5100	2.06	0.840

M_z = Z-average molecular weight (determined by GPC). $\langle r^2\rangle_z{}^{1/2}$ = End-to end distance for HEC at 25 °C.

Celulex-123 (liquid cytolase enzyme, a commercial enzyme from ENMEX S.A.) was used as the degradation agent.

2.2. Methods and instrumentation

2.2.1. Molecular weight measurements

Molecular weights were determined by GPC. A calibration curve was obtained using standards of polymaltriose (PL Laboratories). Studies of GPC were carried out using a Perkin Elmer Model 10 pump, equipped with a Milton-Roy refraction index detector. An array of three columns in series (Microbondagel E500, Microbondagel E125 and Ultrahydrogel TSK gel) was used. HPLC-grade water was used as the mobile phase, which was eluted at a rate of 0.5 ml/min. Sample concentrations of 0.1% (w/v), and injection volumes of 25 μl were used.

2.2.2. Density measurements

Solvent and solution density measurements were carried out using a pycnometer, a milligram balance and a thermometer. A dried and empty pycnometer was weighted, and after that it was filed with the solvent or solution and air bubbles were allowed to rise to the top before inserting the stopper. The system was stabilized at the desired temperature for 30 min, and the pycnometer was weighted again. HEC solution density was calculated from the water density and the weights of solution and solvent at the desired temperature.

2.2.3. Viscosity measurements

Dilute solution viscosity measurements were carried using a Cannon Fenske 100 capillary viscometer. The solutions were prepared from HEC and distilled water, and filtered off through sintered glass before used. Specific viscosity was recorded using the equation:

$$\eta_{\mathrm{sp}} = \frac{\eta - \eta_0}{\eta_0} \qquad (1)$$

where η is the solution viscosity and η_0 the solvent viscosity. Kinetic energy corrections were not made, and solution viscosities were computed as products of flow time and density. Intrinsic viscosities $[\eta]$ were obtained from the plots of $\log(\eta_{\mathrm{sp}}/c)$ versus c (Martin equation) as described previously (Martínez-Richa et al., 1992; Martínez-Richa, 1998)

2.2.4. Enzymatic degradation assay

The hydrolytic action pattern was monitored by measuring the changes in viscosity as a function of incubation time. The enzymatic degradation experiments were carried out at 40 °C, with 0.3% aqueous solutions of HEC at pH 4.5, in a Cannon-Fenske 100 viscometer, as described previously (Martínez-Richa, 1998). Three independent runs were made for each sample. Intrinsic viscosities were determined from plots of η_{sp}/c versus c for measurements made in the same viscometer.

3. Results and discussion

3.1. Calculation of physicochemical parameters

In neutral and acidic aqueous solutions at room temperature, HEC behaves as a highly extended chain. Under basic conditions and in other solvents, HEC attains smaller coil dimensions and higher flexibility. Polymers with lower molecular weights show a more extended configuration. At higher temperatures chain flexibility increases and smaller molecular size are observed. This fact

Table 2
Physicochemical parameters for HEC samples at 40 °C and pH 4.5.

Sample	$[\eta]_{40}$ (dl g^{-1})	$\langle r^2\rangle_{40}{}^{1/2} \times 10^{-3}$ (Å)	$\langle s^2\rangle_{40}{}^{1/2} \times 10^{-3}$ (Å)	$\langle r^2\rangle_{40}{}^{1/2}/\langle r^2\rangle_{25}{}^{1/2}$	$(\langle r_o{}^2\rangle_{40}/DP_z) \times 10^{15}$ (cm)
HEC-1	5.74	1.23	0.50	0.82	54.6
HEC-2	6.42	1.31	0.53	0.83	49.6
HEC-3	7.02	1.41	0.58	0.87	50.3
HEC-4	7.10	1.45	0.59	0.87	50.7
HEC-5	7.60	1.52	0.62	0.88	51.7
HEC-6	8.10	1.56	0.64	0.89	53.3
HEC-7	8.15	1.58	0.65	0.89	52.8
HEC-8	8.35	1.61	0.66	0.89	54.3
HEC-9	8.50	1.63	0.67	0.89	52.7
HEC-10	9.00	1.68	0.69	0.88	55.4
HEC-11	9.32	1.78	0.73	0.89	58.8
HEC-12	9.65	1.81	0.74	0.89	58.7
HEC-13	10.02	1.85	0.76	0.90	58.6
Average				0.88	53.9

$[\eta]_{40}$ = Intrinsic viscosity at 40 °C.

Table 3
Physicochemical parameters for HEC samples at 40 °C and pH 4.5 (continues).

Sample	b, Å	A_m, Å	C_n
HEC-1	23.3	106 (21 monomer units)	20.6
HEC-2	22.3	96 (19 monomer units)	21.4
HEC-3	22.4	98 (19 monomer units)	21.7
HEC-4	22.5	98 (19 monomer units)	21.9
HEC-5	22.7	100 (20 monomer units)	22.3
HEC-6	23.1	104 (21 monomer units)	22.6
HEC-7	22.9	102 (20 monomer units)	22.8
HEC-8	23.3	105 (20 monomer units)	23.4
HEC-9	22.9	102 (20 monomer units)	22.8
HEC-10	23.5	107 (21 monomer units)	23.9
HEC-11	24.2	114 (23 monomer units)	25.4
HEC-12	24.2	114 (23 monomer units)	25.4
HEC-13	24.2	114 (23 monomer units)	25.3
Average	23.2		

b = Effective bond length in Å. A_m = Kuhn–Kuhn equivalent chain segment length C_n = characteristic ratio $\langle h\rangle_0/\mathrm{nl}^2$.

is linked with the negative temperature dependence of $[\eta]$ (Brown et al., 1963).

Using the Flory–Fox Eq. (3), the z-average molecular weights M_z obtained from GPC measurements and the value for α derived using Orofino–Flory equation, root-mean square the end-to-end $\langle r^2\rangle_z{}^{1/2}$ distances at room temperatures for thirteen samples were obtained. Radii of gyration were obtained using the approximation:

$$\langle r^2\rangle_z^{1/2} = 6^{1/2}\langle s^2\rangle_z^{1/2} \tag{16}$$

Results are shown in Table 1.

From the values of $[\eta]_{40}$ and M_z, root-mean square end-to-end distance, radii of gyration and $\langle r_o{}^2\rangle_{40}/DP_z$ for each sample of HEC in water at 40 °C and pH 4.5 were calculated (see Table 2). Other parameters such as the effective bond length b, Kuhn–Kuhn equivalent chain length A_m and characteristic ratio C_n at this temperature were also computed (see Table 3).

Values of characteristic ratio C_n were recorded using Eq. (8), from the corresponding values of DP_z, A_m, b and $\langle r_o{}^2\rangle_{40}$.

3.2. Dependence of root mean square end-to-end distance on degree of polymerization

A plot of $\langle s_o{}^2\rangle^{1/2}{}_{40}$ versus DP_z is shown in Fig. 2. Data was fitted to Eq. (9). A non-linear curve fitting was performed using Origin 6.1 software. Values of 1.87 ± 0.32 and 0.70 ± 0.02 were recorded for parameter b and the Flory exponent ν, respectively of Eq. (8).

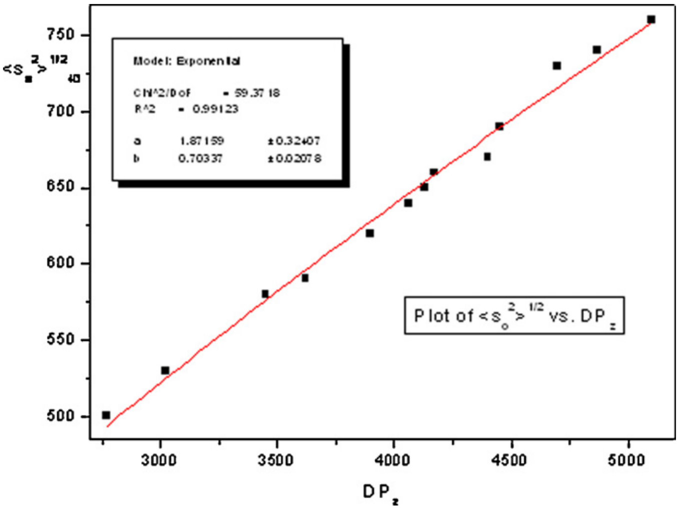

Fig. 2. Plot of $\langle s_o{}^2\rangle_{40}$ versus DP_z for thirteen samples of HEC.

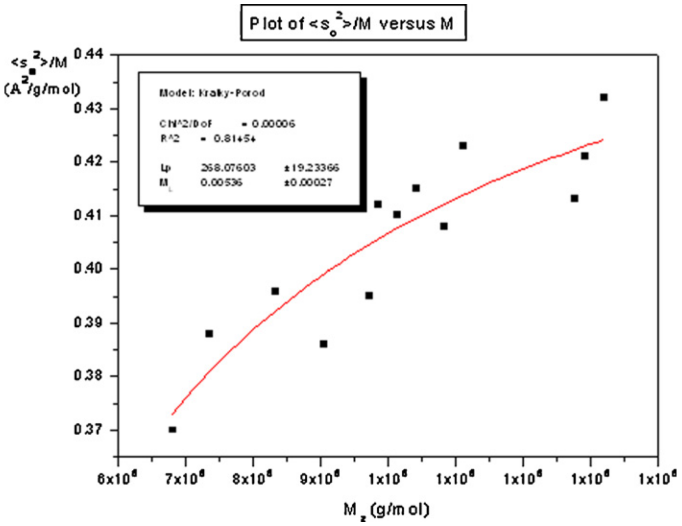

Fig. 3. Kratky–Porod model plot of $\langle s_o{}^2\rangle_{40}/M$ versus $M_z{}^{-1}$ for thirteen samples of HEC.

From Eq. (10) and ν value, we obtain d = 2.3 for HEC at pH 4.5 and 40 °C.

3.3. Estimation of persistence length

Conformation plot of $\langle r_o{}^2\rangle_{40}/M$ versus M is shown in Fig. 3. Curve obtained by least-squares non-linear regression fit to equation 13 is also shown. Values of 268 ± 19 Å and 0.0054 ± 0.0003 g/(molÅ) were recorded for persistence length L_p and m_L, respectively. Using Eq. (14), a value of 350 ± 50 Å was recorded for L_p (see Fig. 4).

A plot of $(M^2/[\eta])$ against $M^{1/2}$ (Eq. (15), YFY model) is linear (see Fig. 5). Correlation coefficient indicates that both variables are linearly associated (r^2 = 0.99). Using A_0 = 0.011, a value of 406 Å was recorded for persistence length L_p. Values recorded for persistence length using different models are shown in Table 4.

3.4. Discussion

Values of $\langle r^2\rangle_z{}^{1/2}$ and $\langle s^2\rangle_z{}^{1/2}$ observed at pH 4.5 and 40 °C are shorter than those observed at room temperature (25 °C) in neutral aqueous solutions for HEC. Molecular sizes under acidic conditions

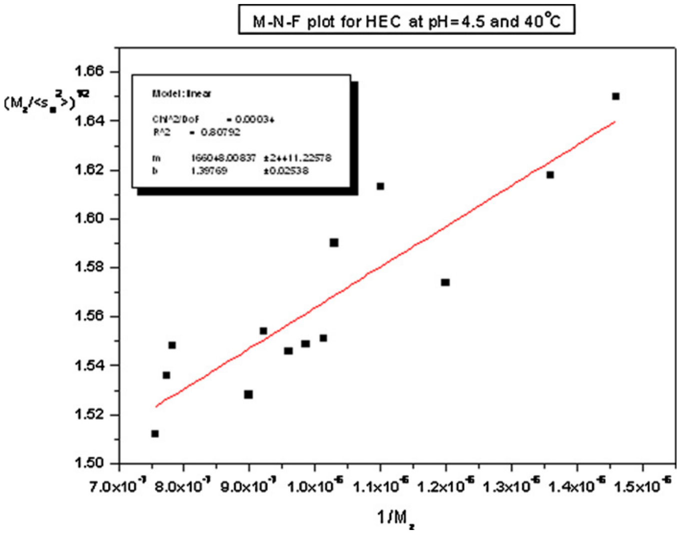

Fig. 4. M–N–F model plot of $[M_z/\langle s_o{}^2\rangle_{40}]^{1/2}$ versus $M_z{}^{-1}$ for thirteen samples of HEC.

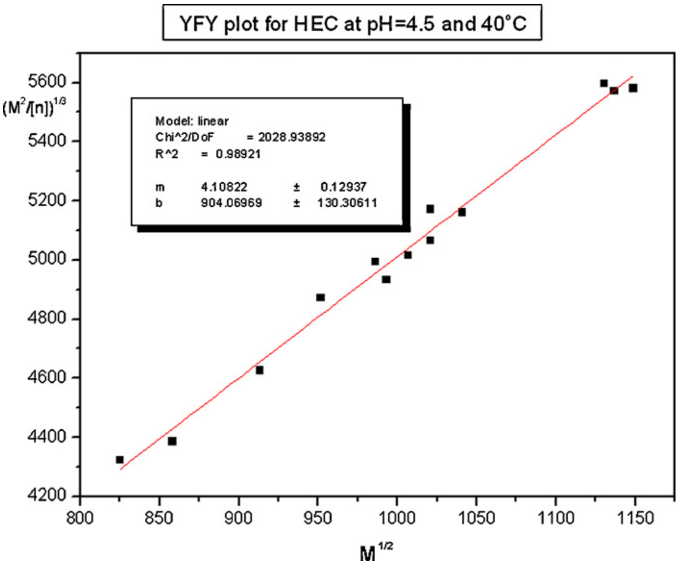

Fig. 5. Y–F–Y model plot of $[M_z{}^2/[\eta]]^{1/3}$ versus $M_z{}^{1/2}$ for thirteen samples of HEC.

at 40 °C are about 82–90% shorter than those observed at room temperature (see column 4 of Table 2). This behavior is in agreement with the negative dependence of molecular size with temperature, and the effect of the acidic medium on the molecular solvent-polymer interactions (Brown et al., 1963).

The value of configurational parameter $\langle r^2\rangle_z/DP_z$ is a function of solvent and temperature (Orofino & Flory, 1957), and is approximately constant for flexible polymers (Brown et al., 1963). For cellulose derivatives, increase in the chain flexibility is reflected in a decreasing value for $\langle r^2\rangle_z/DP_z$ ratio. At pH 4.5 and 40 °C, an average value of 54×10^{-15} cm^2 was recorded for HEC. At room temperature, values of 83 (neutral conditions), 76 (0.5 M NaCl), 63 (0.5 M HCl) and 39 (0.5 M NaOH) $\times 10^{-15}$ cm^2 have been reported (Brown et al., 1963).

As expected, recorded values for effective bond length b are relatively constant. An average value of 23.2 Å is observed for the analyzed samples. For Kuhn–Kuhn equivalent chain segment length A_m, dependence on molecular weight is observed, and they comprise 19–23 monomer units. These values are lower than those reported for HEC in neutral aqueous solution (b = 28Å, A_m = 152Å (30 monomer units)) (Brown et al., 1963), which is expected as lower coil extension and stiffness are observed under acidic conditions and at temperatures higher than 25 °C.

By means of molecular modeling, a value of 36 for characteristic ratio C_n was obtained for cellulose (Brant & Christ, 1990, chap. 4). Values of C_n for HEC are in the range 20.6–25.4, which indicates that a relatively flexible carbohydrate is present at pH 4.5 and 40 °C. However, recorded values are larger than those reported for common polymer–solvent systems (Brandrup & Immergust, 1989; Flory, 1969; Rodríguez, Cohen, Ober, & Archer, 2003).

The recorded values for Flory exponent ν and parameter d indicate that a relatively rigid chain is observed. Both values are different to those expected for a polymer chain following a self-avoiding walk on a two-dimensional surface (ν = 0.75, d = 2).

Table 4
Persistence length for HEC samples at 40 °C and pH 4.5 obtained by different models.

Model	Persistence length L_p, Å
Kratky–Porod	268 ± 19
Murakami, Norisuye and Fujita	350 ± 50
Yamakawa, Fujii and Yoshizak	406

Data dispersion about regression curves using Eqs. (13) (Kratky–Porod model) and (14) (M–N–F model) are observed (see plots in Figs. 3 and 4). Due to this, estimations of persistence length L_p by these models are not accurate. However, estimated values of persistence length L_p are not too different (see Table 4). It is expected that direct solution for persistence length by non-linear regression is more suitable than linear approximation that use ratios of root-mean-square radius and molar mass (Mourey et al., 2005).

The predicted values are higher than those estimated for cellulose and mannan of about 100 Å (Swenson, Schmitt, & Thompson, 1965).

3.4.1. Some considerations on HEC molecular shape

It is well known the tendency of hydroxylakyl celluloses to form rod-like configurations in aqueous systems. This shape persists even in solid films obtained from aqueous solutions (Klemm, Philipp, Heinze, & Wagenknecht, 1998). Measured viscosity depends on solid volume friction (amount of dissipated energy), which is larger for rodlike particle (Boek, Coveney, Lekkerkerker, & van der Schoot, 1997). Intrinsic viscosity [η] is related to the hydrodynamic volume V_h of a polymer with a given conformation. A general expression for this relationship is given by the Einstein–Simha equation:

$$[\eta] = \nu \frac{N_A V_h}{M} \tag{17}$$

The shape factor ν accounts for the effect of geometry in the measured viscosity; ν is equal to 2.5 for spherical shapes and larger for elongated molecules.

If prolate ellipsoids of revolution are considered to geometrically represent rigid polymers, molecular anisotropy can be expressed in terms of the aspect ratio $A = a/b$, where a is the semi-major axis and b is the semi-minor axis (García-Sánchez, Williamson, & Martínez-Richa, 2000). Considering particles performing Brownian motion, Onsager derives the following relationship between intrinsic viscosity and aspect ratio: (Onsager, 1932)

$$[\eta] = \frac{4/15(A)^2}{\ln A} \tag{18}$$

For non-interacting rods with aspect ratio $A = a/b$, Simha (Simha, 1940) and Kuhn and Kuhn (Kuhn & Kuhn, 1945) independently derived the following relationship

$$[\eta] = \frac{A^2}{15[\ln(2A) - 1.5]} + \frac{A^2}{5[\ln(2A) - 0.5]} + C \tag{19}$$

with c = 14/15 (Simha) and 1.6 (Kuhn–Kuhn).

Plots of [η] against A were constructed based on Eqs. (17)–(19), and values of aspect ratios A for each HEC were derived by interpolation. Results are shown in Table 5.

Onsager model predicts higher values of A (in the range 6.3–9.1), whereas values recorded by Simha and Kuhn–Kuhn models are lower (4.9–7.6 for Simha model and 4.3–8 for Kuhn–Kuhn model). These values are close to those reported for derivatives of biphenyl-4-carbonitrile, which are cylinder-shaped liquid crystal molecules (3.5–10) (Villanueva García, Martínez-Richa, & Robles, 2006).

3.5. Mechanistic considerations of enzymatic degradation of HEC

Enzymatic chain hydrolysis assays of celluloses in general take place in dilute aqueous in the pH range 4–9. Enzymatic degradation most common mechanism involves (a) an equilibrium reaction between the enzyme and the substrate to form an enzyme–substrate complex ES and (b) ES decomposition (rate

Table 5
Aspect ratios *a* for HEC samples at 40 °C and pH 4.5 obtained by (A) Onsager (B) Simha and (C) Kuhn–Kuhn models.

SAMPLE	$[\eta]$, (dl g^{-1})	A (Onsager)	A (Simha)	A (Kuhn)
HEC-1	5.74	6.3	4.9	4.3
HEC-2	6.42	6.8	5.5	5
HEC-3	7.02	7.2	6	5.5
HEC-4	7.10	7.2	6.1	5.5
HEC-5	7.60	7.6	6.4	6
HEC-6	8.10	7.9	6.7	6.3
HEC-7	8.15	7.9	6.8	6.3
HEC-8	8.35	8.1	7	6.5
HEC-9	8.50	8.2	7.1	6.6
HEC-10	9.00	8.5	7.4	7
HEC-11	9.32	8.7	7.6	7.2
HEC-12	9.65	8.9	7.8	7.4
HEC-13	10.02	9.1	8	7.6

determining step) leading to a product (P) and the original enzyme (Klemm, Philipp, Heinze, Heinze, & Wagenknecht, 1998; Raff, 2001)

$$E + S \underset{k-1}{\overset{k_1}{\rightleftharpoons}} ES$$

$$ES \xrightarrow{k_2} E + P$$

In the case of cellulolytic enzymes, due to the numerous active protein species present in cellulases, a superposition of different enzymatic chain cleavage mechanisms is present. Other physicochemical factors such as the state of swelling of the substrate are also involved. The particularities of cellulose action have been discussed elsewhere (Klemm et al., 1998). It is expected that tests carried out under homogeneous conditions give more insight into enzymatic action mechanism. However, enzymatic cleavage of cellulose chains can be realized only with water-soluble cellulose derivatives of low or medium degree of substitution (DS).

In a previous work, it was demonstrated by our group that for HEC samples with similar degree of substitution (DS values), resistance toward enzymatic degradation resides on the initial molecular size. A notorious increase in enzymatic resistance is observed when the root-mean square end-to end-distance of the initial substrate is larger than ≈1800 Å (Martínez-Richa, 1998). It is likely that the initial coil dimensions of HEC are also related to a specific association among enzyme, solvent and polymer, which mathematically corresponds to specific enzyme–substrate binding constants (K_m) and/or maximum velocity values ($v_{\max}$).

The geometrical restrictions observed under the experimental conditions used for enzymatic essay determine the mechanism of cellulase action on cellulosic ethers (Martínez-Richa, 1998). A more flexible chain is observed at 40 °C and pH 4.5 with respect to that observed at room temperature, with the consequent decreasing of molecular size. This permits the observation in a more precise way of the differences in enzymatic resistance of cellulosic ethers in a reasonable experimental time.

4. Conclusions

In this work, information based on physicochemical relationships for O-(2-hydroxyethyl)cellulose (HEC) have been derived and examined. The overall results from viscosity and GPC measurements clearly suggest that an elongated geometry, similar to those observed for liquid crystals molecules, is present in aqueous solution of HEC even at 40 °C and pH 4.5.

Besides the need of a better understanding of the actual mechanism operating during the hydrolysis of HEC by cellulases, it is clear that enzyme action occurs on an elongated polymer chain. However, backbone conformation and chain stiffness of HEC is such that chain scission is favored. Conformational changes induced by solution conditions must influence at least secondary and tertiary structure of the carbohydrate. Although surface area for HEC is lower at 40 °C and pH 4.5 (compared to the shape observed at room temperature and under neutral conditions), association between enzyme and HEC and availability of chemical groups where chain scission occurs increases. These residues are now whether more exposed to the solvent or, more possibly, located on the surface of the polymer.

Acknowledgments

Author is especially indebted to Dr. Juvencio Robles (Universidad de Guanajuato) and Dr. Ricardo Vera-Graziano (Universidad Nacional Autónoma de México), who read the manuscript and contributed with their thoughts to the improvement of this manuscript. Their helpful and insightful comments enriched and improved the text. Author also acknowledges Mr. Miguel Angel Delgadillo for GPC measurements and to Karla A. Barrera-Rivera (Universidad de Guanajuato) for her assistance in the preparation of this article.

References

Boek, E. S., Coveney, P. V., Lekkerkerker, H. N. W. & van der Schoot, P. (1997). Simulating the rheology of dense colloidal suspensions using dissipative particle dynamics. *Physical Review E*, *55*(3), 3124–3133.

Bohdanecky, M. (1983). New method for estimating the parameters of the wormlike chain model from the intrinsic viscosity of stiff-chain polymers. *Macromolecules*, *16*, 1483–1492.

Brandrup, J., & Immergust, E. H. (Eds.). (1989). *Polymer Handbook* (p. 33). New York: Wiley-Interscience.

Brant, D. A. & Christ, M. D. (1990). Computer modeling of carbohydrates. In *American Chemical Society, ACS Symposium Series 430* Washington, DC.

Brennan, M. B. (1998). *Chemical and Engineering News*, *76*(12), 39.

Brown, W., Henley, D. & Ohman, J. (1963). Studies on cellulose derivatives. Part II. The influence of solvent and temperature on the configuration and hydrodynamic behaviour of hydroxyethyl cellulose in dilute solution. *Makromolekulare Chemie*, *64*, 49–67.

Cifra, P. (2004). Differences and limits in estimates of persistence length for semi-flexible macromolecules. *Polymer*, *45*, 5995–6002.

de Gennes, P.-G. (1979). *Scaling concepts in polymer physics*. Ithaca, New York: Cornell University Press.

Eisenriegler, E. (1993). *Polymers near surfaces*. Singapore: World Scientific.

Ferenczi, T. A. M. & Cicuta, P. (2005). Shear and compression viscoelasticity in polymer monolayers. *Journal of Physics: Condensed Matter*, *17*, S3445–S3454.

Flory, P. J. (1969). *Statistical mechanics of chain molecules*. New York: J. Wiley and Sons.

Flory, P. J. (1971). *Principles of polymer chemistry*. Ithaca, New York: Cornell University Press.

Flory, P. J. & Fox, T. G. (1951). Treatment of intrinsic viscosities. *Journal of the American Chemical Society*, *73*, 1904–1908.

French, A. D. & Johnson, G. P. (2004). Advanced conformational energy surfaces for cellobiose. *Cellulose*, *11*, 5–22.

French, A. D., Kelterer, A.-M., Johnson, G. P., Dowd, M. K. & Cramer, C. J. (2000). Constructing and evaluating energy surfaces of crystalline disaccharides. *Journal of Molecular Graphics and Modelling*, *18*, 95–107.

García-Sánchez, E., Williamson, D. & Martínez-Richa, A. (2000). Effect of molecular geometry on liquid crystal phase behaviour: Isotropic-nematic transition. *Molecular Physics*, *98*(3), 179–192.

Heine, S., Kratky, O. & Porod, G. (1961). Eine verfeinerte theorie der röntgenkleinwinkelstreuung des verknäuelten fadenmoleküls und ihre anwendung auf cellulosenitrat in lösung. *Makromolekulare Chemie*, *44*, 682–726.

Jaric, M. V. & Tuthill, G. D. (1985). Thermodynamic polydispersity and the Flory exponent. *Physical Review Letters*, *55*, 2891–2894.

Kamien, R. D. (1993). Flory exponents from a self-consistent renormalization group. *Journal de Physique I France*, *3*, 1663–1670.

Katime, I. & Cesteros, C. (2004). *Química Física Macromolecular: II. Disoluciones y Estado sólido*. Bilbao, España: Universidad del País Vasco.

Klemm, D., Philipp, B., Heinze, T., & Wagenknecht, W. (Eds.), (1998). *Functionalization of cellulose* (p. 241). New York: Wiley-VCH.

Klemm, D., Philipp, B., Heinze, T., Heinze, U., & Wagenknecht, W. (Eds.). (1998). *Comprehensive cellulose chemistry vol. 1: Functionalization of cellulose*. (2nd ed., vol. 2, pp. 93–100). New York: Wiley-VCH.

Klop, W. & Kooiman, P. (1965). The action of cellulolytic enzymes on substituted celluloses. *Biochimica et Biophysica Acta*, *99*, 102–120.

Klug, E. D., Winquist, D. P. & Lewis, C. A. (1973). N. M. Bikales (Ed.), *Polymer science & technology: Water soluble polymers* (pp. 401–416). New York: Plenum.

Kuhn, W. & Kuhn, H. (1945). Die Abhängigkeit der Viskositt vom Strömungsgefälle bei hochverdünnten Suspensionen und Lösungen. *Helvetica Chimica Acta*, *28*, 97–127.

Majewicz, T. G., Erazo-Majewicz, P. E. & Podlas, T. J. (2005). *Encyclopedia of polymer science and technology* (2nd ed., vol. 3, pp. 226–269). New York: Wiley.

Martínez-Richa, A. (1998). Variation of intrinsic viscosity in the hydrolisis of hydroxiethylcellulose and its relationship to resistance to enzymatic degradation. *Polymer*, *39*, 3115–3118.

Martínez-Richa, A., Muñoz-Alarcón, H. & Joseph-Nathan, P. (1992). Studies on enzymatic resistance and molecular structure by ^{13}C–NMR of cellulosic ethers. *The Journal of Applied Polymer Science*, *44*, 347–352.

Mazeau, K., Moine, C., Krausz, P. & Gloaguen, V. (2005). Conformational analysis of xylan chains. *Carbohydrate Research*, *340*(18), 2752–2760.

Morgan, P. W. (1946). Industrial and engineering chemistry, analytical edition. *ANCHA*, *18*, 500. ASTM D2364-75.

Mourey, T., Le, K., Bryan, T., Zheng, S. & Bennet, G. (2005). Determining persistence length by size-exclusion chromatography. *Polymer*, *46*, 9033–9042.

Murakami, H., Norisuye, T. & Fujita, H. (1980). Dimensional and hydrodynamic properties of poly(hexyl isocyanate) in hexane. *Macromolecules*, *13*, 345–352.

Onsager, L. (1932). Viscosity and particle shape in colloid solutions. *Physical Reviews*, *40*, 1028.

Orofino, T. A. & Flory, P. J. (1957). Relationship of the second virial coefficient to polymer chain dimensions and interaction. *Journal of Chemical Physics*, *26*, 1067–1076.

Raff, L. M. (2001). *Physical chemistry*. New Jersey: Prentice Hall., pp. 1131–1133.

Rodríguez, F., Cohen, C., Ober, C. K. & Archer, L. A. (2003). *Principles of polymer systems*. New York-London: Taylor and Francis. Chapter 7.

Roesser, D. S., McCarthy, S. P., Gross, R. A. & Kaplan, D. L. (1996). Effects of substitution site on acetyl amylose biodegradability by amylase enzymes. *Macromolecules*, *29*, 1–9.

Saito, H., Tuzi, S. & Naito, A. (1998). Polysaccharides and biological systems. In *Solid state NMR of polymers*. New York: Elsevier., pp. 891–921.

Simha, R. (1940). The influence of brownian movement on the viscosity of solutions. *Journal of Physical Chemistry*, *44*, 25–34.

Sun, S. F. (2004). *Physical chemistry of macromolecules: Basic principles and issues* (2nd ed.). New York: Wiley.

Swenson, H. A., Schmitt, C. A. & Thompson, N. S. (1965). *Journal of Polymer Science Part C: Polymer Letters*, 243–252.

Tatek, Y. B. & Slater, G. W. (2006). A simulation model of biofilms with autonomous cells: I. Analysis of a two-dimensional versión. *Physica A: Statistical Mechanics and its Applications*, *362*(2), 382–402.

Teraoka, I. (2002). *Polymer solutions: An introduction to physical properties*. New York: Wiley.

Tezuka, Y., Imai, K., Oshima, M. & Chiba, T. (1989). Determination of substituent distribution in cellulose ethers by means of a ^{13}C nuclear magnetic resonance study on their acetylated derivatives: 3. Hydroxyethylcellulose. *Polymer*, *6*, 2288–2291.

Tonelli, A. E. (2001). *Polymers from inside out*. New York: Wiley.

Tümmler, B., Maass, G., Weber, E., Wehner, W. & Vögtle, F. (1977). Noncyclic crown-type polyethers, pyridinophane cryptands, and their alkali metal ion complexes: synthesis, complex stability, and kinetics. *Journal of the American Chemical Society*, *99*, 4683–4690.

Villanueva García, M., Martínez-Richa, A. & Robles, J. (2006). Derivation by electronic structure calculation of the aspect ratios (length/diameter) for homologous series of calamitic liquid crystals. *Molecular Crystals and Liquid Crystals*, *446*, 245–254.

Wirick, M. G. (1968). A study of the enzymic degradation of CMC and other cellulose ethers. *Journal of Polymer Science Part A: Polymer Chemistry*, *6*, 1705–1718.